Article

Co-delivery of doxorubicin and shAkt1 by poly(ethylenimine)-glycyrrhetinic acid nanoparticles to induce autophagy-mediated liver cancer combination therapy

Feng-zhen Wang, Lei Xing, Zheng-Hai Tang, Jin-Jian Lu, Peng-Fei Cui, Jian-Bing Qiao, Lei Jiang, Hu-Lin Jiang, and Li Zong

Mol. Pharmaceutics, **Just Accepted Manuscript** • DOI: 10.1021/acs.molpharmaceut.5b00879 • Publication Date (Web): 19 Feb 2016

Co-delivery of doxorubicin and shAkt1 by poly(ethylenimine)-glycyrrhetinic acid nanoparticles to induce autophagy-mediated liver cancer combination therapy

Feng-Zhen Wang[a,d,1], Lei Xing[a,1], Zheng-hai Tang[c], Jin-Jian Lu[c], Peng-Fei Cui[a], Jian-Bing Qiao[a], Lei Jiang[a], Hu-Lin Jiang[a,b,*] and Li Zong[a,*]

[a] State Key Laboratory of Natural Medicines, Department of Pharmaceutics, China Pharmaceutical University, Nanjing 210009, China

[b] Jiangsu Key Laboratory of Drug Discovery for Metabolic Diseases, China Pharmaceutical University, Nanjing 210009, China

[c] State Key Laboratory of Quality Research in Chinese Medicine, Institute of Chinese Medical Sciences, University of Macau, Macao, China

[d] Department of Pharmaceutics, The Affiliated Hospital of Xuzhou Medical College, 99 West Huaihai Road, Xuzhou, 221002, Jiangsu, China

[*] To whom correspondence should be addressed.

Professor Hu-Lin Jiang, State Key Laboratory of Natural Medicines, Department of Pharmaceutics, China Pharmaceutical University, Nanjing 210009, China

Tel: +86-25-83271027; Fax: +86-25-83271027; E-mail: jianghulin3@163.com

Professor Li Zong, Department of Pharmaceutics, China Pharmaceutical University, Nanjing 210009, China

Tel: +86-25-83271317; Fax: +86-25-83271335; E-mail: zong216@yahoo.com.cn

[1] These authors contributed equally to this work.

ABSTRACT: Combination therapy has been developed as a promising therapeutic approach for hepatocellular carcinoma therapy. Here we report a low toxicity and high performance nanoparticle system that was self-assembled from a poly(ethylenimine)-glycyrrhetinic acid (PEI-GA) amphiphilic copolymer as a versatile gene/drug dual delivery nanoplatform. PEI-GA was synthesized by chemical conjugation of hydrophobic GA moieties to the hydrophilic PEI backbone via an acylation reaction. The PEI-GA nanocarrier could encapsulate doxorubicin (DOX) efficiently with loading level about 12 %, and further condense DNA to form PEI-GA/DOX/DNA complexes to co-deliver drug and gene. The Diameter of the complexes is 102 ± 19 nm with zeta potential of 19.6 ± 0.2 mV. Furthermore, the complexes possess liver cancer targeting ability and could promote liver cancer HepG2 cell internalization. Apoptosis of cells could be induced by chemotherapy of DOX and PI3K/Akt/mTOR signaling pathway acts a beneficial effect on the modulation of autophagy. Here, it is revealed that utilizing PEI-GA/DOX/shAkt1 complexes results in effective autophagy and apoptosis, which is useful to cause cell death. The induction of superfluous autophagy is reported to induce type-Ⅱ cell death and also could increase the sensity of chemotherapy to tumor cells. In this case, combining autophagy and apoptosis is meaningful for oncotherapy. In this study, PEI-GA/DOX/shAkt1 has demonstrated favorable tumor target ability, little side effects and ideal antitumor efficacy.

KEYWORDS: combination therapy, self-assembled, glycyrrhetinic acid, liver cancer targeting, autophagy.

INTRODUCTION

Hepatocellular carcinoma (HCC) is the second most lethal disease and the incidence of HCC is increasing worldwide.[1] Doxorubicin (DOX) is a widely used chemotherapeutic drug for treatment of HCC. However, previous studies indicated that various mechanisms could be developed to decrease the sensitivity of cancer cells to DOX,[2, 3] which leads to the reduction of drug potency and remains a formidable challenge in the use of DOX in clinic.[4] Combination therapy and co-delivery of gene/drug system through synergistic and enhancement effect are now becoming a prospective approach for cancer therapy.[4-10]

To our knowledge, the emergence of HCC is associated with the activation of the PI3K/Akt/mTOR signaling pathway.[11, 12] Akt, as a key factor in the pathway, facilitates the development of tumor cell proliferation, angiogenesis, metastasis and invasion. In addition, it occupies an important position in the increase of tumor resistance to chemotherapy and inhibition of tumor cell apoptosis.[13, 14] The signaling of PI3K/Akt/mTOR also mediates an effect on the modulation of autophagy and inhibition of the pathway might induce superfluous autophagy, which could induce type-Ⅱ cell death. With the improved understanding of cancer at the molecular level, a shRNA silencing Akt1 (shAkt1), as a therapeutic gene, has been widely studied.[15, 16] It not only could confer the sensitivity of chemotherapeutics to tumor cells in apoptosis competent cancer cells, but also could regulate cancer cell death through superfluous autophagy in apoptosis-defective cells.[13, 14, 17, 18] It is well-known that apoptosis and autophagy, through which cells self-regulated cell death, are both intimately related to cancer cell growth and were reported to be effective targets for the treatment of cancer.[19] Induction of apoptosis and autophagy has been evaluated as a promising approach for interfering with the growth of cancer cells. Therefore, the combination therapy of DOX and shAkt1 was investigated in the study.

To achieve the successful co-delivery of DOX and shAkt1, it requires the development of efficient and safe delivery vehicles.[20, 21] As a promising polycationic vector, poly(ethylenimine) (PEI) is often applied as a “golden standard” of polycation due to its properties of highly positive charge to condense and protect gene from

nuclease degradation as well as "proton sponge effect" to facilitate endosomal release of gene.[22] Another important advantage of PEI is its high density of primary amines in the structure, making it easy to chemical modification.[23-25] However, its high cytotoxicity remains a great challenge in clinical application. By comparison, PEIs with low molecular are safer to use, yet their comparatively low transfection efficiency has limited their applications. To circumvent the problems associated with low molecular weight, one rational strategy is to graft hydrophobic units on the backbone of PEI. PEIs with the modification of hydrophobic anchors could cause the reduction of the cytotoxicity of PEI by decreasing its high charge density. Besides, it also could spark the increasement of transfection efficiency by modulating the complex interactions with cells (facilitating adsorption on cell surfaces and cell uptake). For instance, Bhattacharya *et al*. reported that lipopolymer based on low molecular weight PEI and cholesterol had a higher transfection efficiency and better serum stability than commercially available PEI25k.[26] Liu reported that PEI with the modification of hydrophobic anchors, such as fatty acids, lithocholate, cholesterol or Vitamin E, could increase the transfection efficiency of siRNA.[27] Park reported that trans-retinoic acid was grafted to PEI to synthesize a new polymer as gene carrier and it showed less cytotoxicity and better characteristics than PEI without modification.[28] These aforementioned results suggest that the means of modification of PEI should be a promising method either to decrease its cytotoxicity or to increase its transfection efficiency .[23-28] As a metabolite of the natural product glycyrrhizin, glycyrrhetinic acid (GA) is a preferential candidate as hydrophobic unit (lgP = 4.69)[29] and could be linked to a low molecular PEI. PEI with the modification of GA might achieve the possibility of liver targeted delivery because of the targeting ability of GA to liver tumor.[25] In addition, amphiphilic derivative with GA conjugation could form nano-sized self-aggregates for the delivery of hydrophobic drug.[30] The construction of PEI-GA nanoparticle might be used as an excellent drug and gene carrier.

Herein, we successfully fabricated and synthesized a series of poly(ethylenimine)-glycyrrhetinic acid (PEI-GA) copolymers. PEI-GA could self-assemble into nanostructure. GA hydrophobic domain could load hydrophobic

anticancer drug through the hydrophobic interaction and the modification of GA also increased transfection activity and ensureed its effective delivery because of the targeting property of GA to HepG2 cells.[23-25, 29, 30] PEI was used as an efficient gene carrier to deliver shAkt1. This nanoparticle could co-deliver DOX and shAkt1 into the same cell and achieve the synergistic/combined anti-tumor effect. Their physicochemical properties, *in vitro* cytotoxicity, intracellular distribution, cellular apoptosis and autophagy, and *in vivo* antitumor efficacy in xenograft mice model were investigated in detail.

Materials and methods

Materials. N-hydroxysuccinimide (NHS), N,N′-dicyclohexylcarbodiimide (DCC) and GA were purchased from Sigma-Aldrich (St. Louis, MO, USA). Branched PEI (25, 10, 3.5, 1.8 and 0.6 kDa) were bought from Wako (Osaka, Japan). Doxorubicin hydrochloride (DOX·HCl, purity > 98 %) was bought from Alliance Bernstein Technology Co., Ltd. (Beijing, China). 3-(4, 5-dimethylthiazol-2-yl)-5-(3-carboxymethoxyphenyl)-2-(4-sulfophenyl)-2H-tetrazolm (MTS) was bought from promega (promega, USA). Dulbeco`s modified eagle medium (DMEM) was purchased from Gibico BRL (Paris, France). Fetal bovine serum (FBS) was obtained from HyClon (Logan, Utah, USA). All other chemicals were used with reagent grade or higher. Plasmids used in this study were generated in *Escherichia coli*, then withdrew by the alkali lysis technique, and finally purified by a E.Z.N.A.®Fastfilter Endo-free Plasmid Maxi kit (Omega, USA). Sequence of the targeted Akt1 mRNA was GAAGGAAGTCATCGTGGCC and the corresponding cassette of oligonucleotide specific to the mRNA was designed.

Cell culture. HepG2 and Hepa-1.6 cells were obtained from the Chinese Academy of Sciences cell bank. Cells were cultured in DMEM medium supplemented with 10 % FBS at 37 ^{o}C in 5 % CO_2 atmosphere.

Animals. C57BL/6J mice (male, six-week-old, 20 ± 2 g) were bought from the Model Animal Research Center of Nanjing University (Nanjing, China) and kept in the animal room with the temperature and relative humidity controlled, under a 12 h light/dark cycle. The mice were used in accordance to the policy and regulations for

the care and use of laboratory animals of China Pharmaceutical University.

Synthesis and characteristics of PEI-GA copolymer. The synthesis route of PEI-GA copolymer is presented in Figure. 1a. The GA moiety was conjugated to PEI with amide linkage through the reaction of primary amines of PEI with carboxyl groups of GA in DMSO in the presence of NHS. The characteristic of the PEI-GA copolymer was analyzed by ^{1}H nuclear magnetic resonance (^{1}H NMR) (Avance™ 600, Bruker, Germany), UV scanning spectra (Thermo, Bruker, China) and Fourier-transform infrared spectrometer (FT-IR) (Tenson, Bruker, Germany).

The buffering capability of PEI-GA copolymer was mensurated by acid-base titration with the pH ranging from 10.0 to 4.0. Briefly, 2 mg of PEI-GA copolymer were dispersed in 10 mL of 150 mM NaCl solution under shaking. The solution was adjusted to an initial pH of 10.0 with 0.1 M NaOH. It was then dropwised with 0.1 M HCl and the pH was monitored using a pH meter (OHAUS, USA). PEI-25kDa was used as a control.

The molecular weight of PEI-GA was analyzed by a gel permeation chromatography column coupled with multi-angle laser scattering (GPC-MALS) with 690 nm laser wavelength (Dawn Eos, Wyatt, USA). Chloroform was used as a mobile phase and the flow rate was 1.0 ml/min. The column temperature was maintained at 40 °C. Polystyrene with average molecular weights ranging from 1.0×10^3 to 9.5×10^3 Da were used as standards for calibration.

Preparation and characterization of PEI-GA/DOX/shAkt1 nanoparticles. As a first-line therapy for HCC, hydrophobic DOX was used for a model drug. It might be loaded into the lipophilic cores during the self-assembly process of PEI-GA using a dialysis method and shAkt1 could be bound to the cationic backbone of the resulting DOX-loaded nanoparticles (Scheme 1a). Briefly, DOX·HCl (100 mg) was stirred with TEA (3-fold molar of DOX·HCl) in 15 ml DMSO to obtain DOX base. PEI-GA (100 mg) were dispersed in another 15 ml DMSO (30 ml for blank PEI-GA). The DOX base solution was then added and mixed with the DMSO solution. Subsequently, 10 ml deionized water was added to the mixture by dripping slowly. The obtained solution was vigorously stirred for 2h. Afterwards, the solution was transferred into a

dialysis bag (MWCO = 3500) and dialyzed against deionized water. The outer phase was tipped away and fresh deionized water was added at 4, 8, 12, 18, 24, 36, 48 and 60 h. After 60 h, the solution inside the dialysis bag was recovered, and filtered. For prepare PEI-GA/shAkt1 or PEI-GA/DOX/shAkt1 nanoparticles, PEI-GA or PEI-GA/DOX solutions were further incubated with shAkt1. Then PEI-GA, PEI-GA/DOX, PEI-GA/shAkt1 and PEI-GA/DOX/shAkt1 nanoparticles were lyophilized. The powders produced were stored at -20 ^{o}C until use.

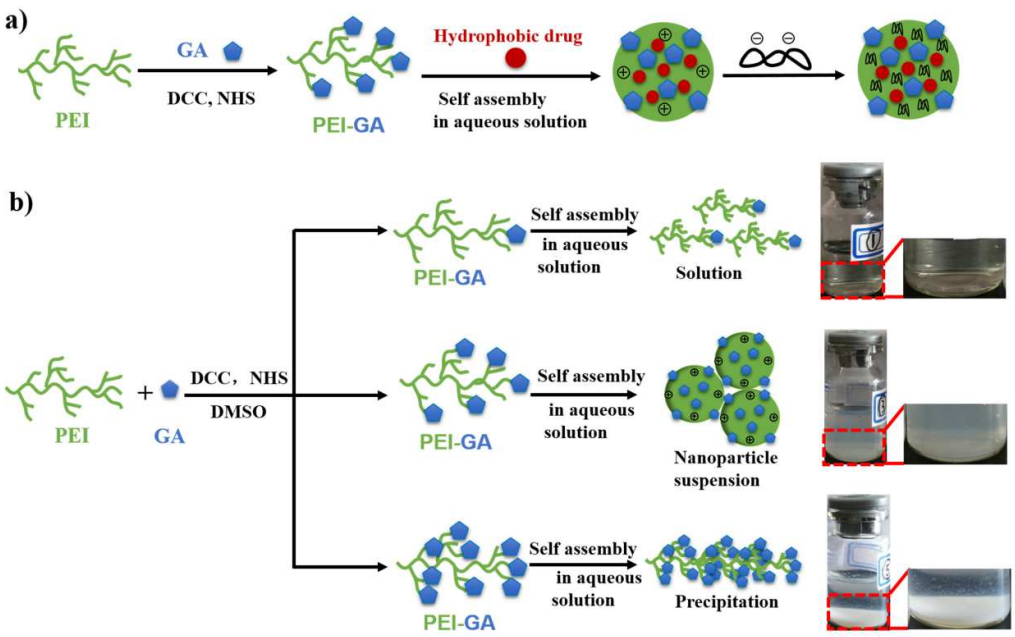

Scheme 1. (a) A schematic diagram of PEI-GA/DOX/DNA nanoparticles' formation. (b) Schematic illustration of PEI-GA nanoparticle formation with different GA grafted ratios.

The critical aggregation concentration (CAC) serves as an important indicator of nanoparticle stability. In this study, the CAC of PEI-GA was measured using the fluorescence probe technique with pyrene as the probe. Emission spectra of pyrene incubated with different concentrations of PEI-GA (ranging from 1 to 1000 μg/mL) were observed by fluorescence spectroscopy (SpectraMax M5, Molecular Devices) with excitation wavelength at 334 nm. The intensity ratio between the third peak (382 nm) of emission wave length and the first peak (371 nm) (intensity ratio, I_{382}/I_{371}) was

determined for each sample in triplicate.

The average particle size, polydispersity index (PI) and zeta-potential measurements were made using a ZetaPlus particle size and zeta potential analyzer (Brookhaven Instruments, USA). The morphology of blank PEI-GA and PEI-GA/DOX/shAkt1 nanoparticles were examined by EF-TEM (LIBRA 120, Carl Zeiss, Germany). The entrapment efficiency (EE %) of DOX was acquired by measuring the DOX encapsulated in assembled nanoparticles against that added in fabrication. The drug loading (DL %) was obtained as the ratio between the mass of DOX encapsulated and that of the DOX-loaded nanoparticles. The concentration of DOX was calculated according to a standard curve by UV/vis spectrophotometry (UV-2450, Shima-dzu, Japan) at 480 nm.

The gel retardation assay. PEI-GA/DNA and PEI-GA/DOX/DNA complexes were prepared freshly before use at various N/P ratios from 0.1 to 20 with 12 μL final volume. Luciferase-encoding plasmid DNA (pGL3) was used. The complexes including loading dye mixture were loaded on a 1 % agarose gel with Goldview staining and run with Tris-acetate (TAE) buffer at 100 V for 30 min. The location of the DNA was captured through gel image system (Tanon 1600, China).

Protection and release properties of DNA in PEI-GA/DOX/DNA nanoparticles were analyzed electrophoretically by the method of Jiang *et al*.[32] Briefly, DNase I or PBS in DNase I/Mg^{2+} digestion buffer with the volume of 1 μL was added to 4 μL of complexes solution (N/P ratio: 5:1) or to 0.4 μg of naked plasmid DNA. The mixed solutions were incubated at 37 ^{o}C with continuous stirring at 100 rpm for 30 min. Then all mixtures were maintained with 4 μL EDTA (250 mM) for 10 min at 65 ^{o}C for DNase I inactivation. Afterwards, the samples were mixed with 1 % sodium dodecyl sulfate (SDS) dispersed in 1 M NaOH at a final volume of 18 μL. The samples finally were incubated for 2 h at room temperature, and were run electrophoretically in 1 % agarose gel with TAE running buffer for 40 min at 50 V.

Release of DOX and DNA *in vitro*. The *in vitro* DOX and DNA release from PEI-GA/DOX/DNA nanoparticles was investigated. Briefly, 1 mg/mL PEI-GA/DOX/DNA nanoparticles dispersed in PBS buffer (pH 7.4) were placed in a

dialysis bag (MWCO = 1000). The bag was suspended in 50 mL PBS buffer at 37 ^{o}C with shaking speed of 100 rpm. At indicated time, 1 mL of the release medium was withdrawn and fresh PBS buffer was added. The DOX and DNA content in the samples were quantified spectrophotometrically by determining the absorbance at 480 and 260 nm, respectively. The experiment was performed in triplicate.

Cellular uptake. Intracellular location of DOX was monitored by fluorescent inverted microscope (Nikon ti-s, Japan). HepG2 cells were plated in a 6-well plate at a density of 30×10^4 cells with 2 mL growth medium for 18 h in a 5 % CO_2 incubator at 37 ^{o}C to allow the cells to adhere. The medium were then respectively renewed by the medium containing PEI-GA/DOX/DNA complexes, the combined of GA and PEI-GA/DOX/DNA complexes, or only DOX, respectively at a DOX concentration of 1 μg/well. After treatment for 6 h, the cells were immediately washed three times with PBS. Then cell fluorescence was analyzed.

To measure the fluorescence intensity, the detached and adherent cells were washed three times with PBS and further collected by trypsinization. The cells were then resuspended in PBS. The mean fluorescence intensity at 488/590 nm of DOX was analyzed using flow cytometer (BD Accuri C6, USA).

In vitro cytotoxicity. To assess the cell proliferation, MTS assay was performed. HepG2 cells were plated at a density of 1×10^4 with 200 μL growth medium per cell in 96-well plates at 37 ^{o}C under 5 % CO2 for 18 h. Then the cells were incubated with the culture media containing saline, PEI-GA, DOX, PEI-GA/DOX, and PEI-GA/DOX/shAkt1 complexes at different concentrations (0, 5, 10, 20, and 50 μg/mL), respectively. Each experiment was performed in triplicate. After treatment for 24 h, the MTS solution (20 μL) was added to each well and the cells were incubated for another 4 h at 37 ^{o}C. The formazan crystals were dispersed in the meida by agitating the 96-well plates on an orbital shaker. The optical density values were measured in each well by a microplate reader (Thermo Scientific Multiskan GO, USA) at the absorbance of 490 nm. The Bliss method was applied to measure the half maximal inhibitory concentration (IC_{50}).

Cellular apoptosis and autophagy. HepG2 cells plated in 6-well plates were

incubated for 24 h at 37 ^{o}C with saline, PEI-GA, DOX, PEI-GA/DOX or PEI-GA/DOX/shAkt1 complexes to evaluate the antitumor efficiency. Annexin V and Propidium Iodide (PI) double staining were used to detect cells apoptosis by flow cytometry (BD Accuri C6, USA) using the Annexin V-FITC apoptosis detection kit I. For autophagy investigation, transfected cells were washed thrice with ice-cold PBS. Cells were lysed on ice for 30 min and meanwhile vortexed every 5 min. The lysates were centrifuged for 5 min at 10000 rpm at 4 ^{o}C, and then detected by Western blot analysis. Protein concentration was measured using a BCA Protein Assay Kit according to the manufacturer's instructions. Total protein (30 μg) was subjected to electrophoresis in 12 % Bis-Tris-polyacrylamide gels. Following electrophoresis, the proteins were transferred to Immobilon Transfer Membranes (Millipore, Bedford, USA) at 300 mA for 45 min. The membranes were then incubated with 5 % BSA in PBS for 1 h and subsequently incubated with 1 % BSA in PBS with primary antibodies against Akt1, LC3B-I and LC3B-II (1:1000) (Santa Cruz Biotech., Santa Cruz, USA) at 4 ^{o}C overnight. The membranes were washed thrice in TBST and further incubated in 1 % BSA with horseradish peroxidase-conjugated donkey anti-goat serum (1:10000) (Santa Cruz Biotech., Santa Cruz, USA) for 45 min. The immune complexes were visualized using the ECL system (Pierce, Rockford, USA). The relative levels for Akt1, LC3B-I and LC3B-II protein were normalized to the levels of β-actin.

Hemolysis test and systemic toxicity. The rabbit red blood cells (RBC) in heparin sodium-containing tubes were collected by centrifugation at 2500 rpm for 10 minutes and washed thrice with physiological saline. After rinsing, the RBC were dispersed in physiological saline at the concentration of 2 % (w:v). Different amounts of PEI-GA/DOX/shAkt1 nanoparticles were resuspended in physiological saline and incubated with the equal volume of 2 % RBC solutions. Following incubation for 1 h at 37 ^{o}C, the samples were centrifugated at 3000 rpm for 5 min. The supernatant (200 μL) was added in 96-well plate and the absorbance of sample (A_s), negative (A_n) and positive controls (A_p) were analyzed for released hemoglobin at 540 nm using ThermoMultiskan GO (Thermo Scientific, USA). 1 % Triton X-100 and physiological

saline solutions were applied as positive and negative control, respectively. Percentage hemolysis of RBC was computed according to the following formula: $[(A_s-A_n) / (A_p-A_n)] \times 100$ %.

In vivo antitumor efficacy in xenograft model mice. C57BL/6J mice (six-week-old, male) were randomly divided into 5 groups with 6 mice in each group: 1) saline; 2) DOX (10 mg/kg); 3) PEI-GA (10 mg/kg); 4) PEI-GA/DOX (10 mg/kg); 5) PEI-GA/DOX/shAkt1 (10 mg/kg). After 14 days of Hepa-1.6 cells (1×10^7) implantation, the mice were used and treatment groups were administrated via tail vein twice a week. Tumor growth was recorded by measuring length (l) and width (w) and the volume (mm^3) was computated according to the following formula: $V = lw^2/2$. The survival rates and body weights were monitored throughout the study.

Statistical analysis. Experiments were performed at least three times in a parallel manne and all data were expressed as means ± standard deviation (SD). Statistical analysis was performed using SPSS 19.0. Comparisons were performed using the ANOVA-test to determine whether data groups differed significantly from each other. Statistically significant difference was considered at *P*-values< 0.05.

RESULTS AND DISCUSSION

Formation and characterization of PEI-GA, PEI-GA/DOX and PEI-GA/DOX/shAkt1 nanoparticles. The characteristics of PEI-GA were verified by UV scanning spectra, ^{1}H NMR and FT-IR (Figure. 1b, 1c and 1d, respectively). As displayed in Figure. 1b, the appearance of the UV absorbance peak of GA in PEI-GA was demonstrated to the successful graft of GA on PEI backbone. The proton peaks of PEI (–$NHCH_2CH_2$–) showed at 2.0-0.6 ppm and the proton peaks of GA at 3.5-2.5 ppm indicated that GA was introduced to the PEI chain (Figure. 1c). Moreover, the FT-IR peak of -CO-NH- at 1651 and 1541 cm^{-1} (Figure. 1d) in PEI-GA, further indicated the successful synthesis of PEI-GA. In order to synthesis PEI-GA copolymers with different modification of GA, we make a series of reaction of PEI and GA with different feed ratio. The quantity of GA in the copolymer of PEI-GA was detected by UV and the degree of GA grafting was between 15-75 % (Table 1).

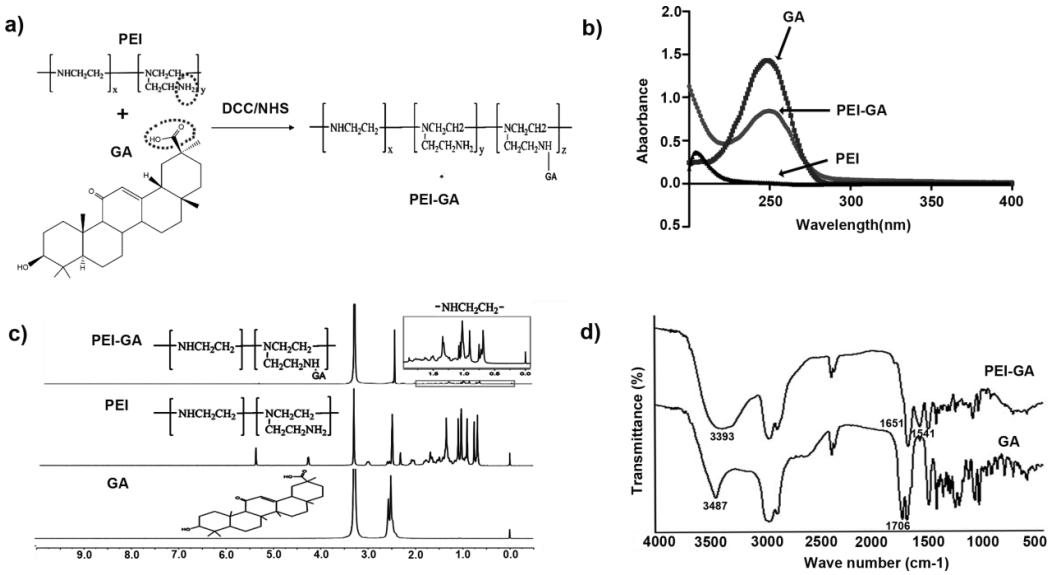

Figure. 1. (a) Synthesis of PEI-GA. Characterizations of PEI-GA, GA, and PEI via (b) the ultra violet; (c) ^{1}H NMR in *d* 6-DMSO; and (d) IR.

As shown in Table 1, the critical association concentrations (CAC) of PEI-GA became lower with the increase of the graft ratio of GA and the decrease of the molecular weight of PEI. Owing to the high amount of amino groups on PEI-GA nanoparticle surface, all of the nanoparticles were positively charged, with charge decreasing as graft ratio of GA increased (Table 1). As shown in Scheme I (b), more aggregation was observed with the increasing grafting ratio of GA. The sizes of the formed nanoparticles ranged between 60 nm and 250 nm with narrow size distributions (PI < 0.25). Conventional acid-base titration was applied to investigate the buffering capacity of PEI-GA. PEI-GA with different graft ratios of GA exhibited nearly the same buffering capacity over the pH range 7.4 to 5.1 (14.3-14.8 %). For the successful formation of nanoparticles using PEI-GA copolymer, the most important prerequisite was to control the graft ratio of GA. PEI-GA with either low graft ratio or high graft ratio of GA were hard to self-assemble into nanoparticles in water. Yet PEI-GA with suitable graft ratio (Table 2) of GA can easily self-assemble into nano-aggregates based on the interaction of functional groups among GA. The CAC is well-controlled by the molecular weight of PEI and the GA graft ratio. $PEI_{3.5k}$-$GA_{1/2}$ with the lowest CAC (22.94 $\mu g \cdot mL^{-1}$) is selected for further study as it is easy to self-assemble into nanoparticles in water and could keep stable for a long

time (more than one year). The molecular weight of $PEI_{3.5k}$-$GA_{1/2}$ was 7.27 kDa with 1.41 polydispersity index determined by GPC measurement.

Table 1

Physicochemical properties of synthesized PEI-GA.

Type of PEI-GA	graft ratio (%)	CAC ($\mu g\ mL^{-1}$)	particle size (PI) (nm)	Zeta Potential (mV)
PEI(1.8k)-GA(1/4)	21.6	38.63	67.4 (0.21)	28.3
PEI(1.8k)-GA(1/2)	43.4	-	-	-
PEI(1.8k)-GA(1/1)	51.9	-	-	-
PEI(3.5k)-GA(1/4)	19.6	46.82	91.2 (0.13)	29.6
PEI(3.5k)-GA(1/2)	38.9	22.94	60.7 (0.19)	19.9
PEI(3.5k)-GA(1/1)	47.5	-	-	-
PEI(10k)-GA(1/4)	18.8	79.32	110.5 (0.16)	37.3
PEI(10k)-GA(1/2)	32.1	54.16	96.4 (0.22)	25.7
PEI(10k)-GA(1/1)	40.2	28.28	89.7 (0.17)	16.3
PEI(25k)-GA(1/4)	16.8	103.83	243.9 (0.19)	30.8
PEI(25k)-GA(1/2)	29.4	68.81	162.5 (0.21)	24.2
PEI(25k)-GA(1/1)	44.7	35.83	113.7 (0.23)	15.7

To illustrate the detailed surface chemical composition of PEI-GA nanoparticles, X-ray photoelectron spectroscopy (XPS) was performed. The data indicated that GA is shown on the surface of our prepared PEI-GA nanoparticles (Table 2). A similar result was obtained by Zhang *et al*.[24] GA on the surface of nanoparticles is beneficial to achieve the targeting efficiency to hepatocyte as the GA receptors of the liver.[33, 34] Transmission electron microscopy (TEM) image indicated that the DOX-loaded PEI-GA/DNA complexes still exhibited spherical morphology with good monodispersity (Figure. 2a), suggesting that DOX-loaded PEI-GA/DNA complexes did not collapse when DNA is combined. The encapsulation efficiencies (EE) were measured by fluorescence spectra. As a modular system, DOX loading can be easily achieved and an obvious increase in DOX loading was observed with the increase

graft amount of GA as shown in Figure. 2b. The maximum drug loading (DL) could reach about 15 %, which may attribute to the hydrophobic interaction between GA and DOX. To clarify the structural integrity of DOX-loaded PEI-GA/DNA complexes when DNA is combined, the aggregation behavior of PEI-GA was investigated by fluorescence spectrophotometer using pyrene as a probe. The intensities of the emission wavelength at 372 and 383 nm were monitored. The ratios of I_{372}/I_{383} of various samples are shown in Figure. 2c. A lower ratio would be obtained if pyrene was encapsulated in a more hydrophobic core. In this study, the ratio of I_{372}/I_{383} decreased when pyrene was encapsulated in the PEI-GA nanoparticles. Besides, the ratio further decreased when the DNA is combined to PEI-GA/pyrene nanoparticles, suggesting that pyrene was still in the core of PEI-GA/pyrene /DNA complexes even if DNA is combined. These data demonstrated that the PEI-GA nanoparticles was efficient for both drug and gene delivery.

The condensability of DNA is required for polycationic vectors to effectively achieve gene expression in target cell.[34-36] The DNA binding ability of PEI-GA or PEI-GA/DOX was investigated by gel retardation assay. As indicated in Figure. 2d, either PEI-GA or PEI-GA/DOX was capable to bind DNA efficaciously, and the intensity of the uncomplexed DNA band disappeared at N/P 1 and 2, respectively. Higher N/P ratio was needed for PEI-GA/DOX, which may be related with the lower zeta potential of PEI-GA/DOX (data not shown).

Table 2

XPS analysis of PEI-GA nanoparticle

Sample	XPS elemental ratios (%)			XPS N_{1S} envelope ratios (%)		XPS O_{1S} envelope ratios (%)		
				N-C	N-O-C=O	O-C=O	C=O	O-C
	C	O	N	Bingding Energy (eV)				
				399.41	403.00	531.97	533.90	535.08
PEI-GA	76.15	19.24	4.61	28.62	71.38	23.31	11.09	65.6

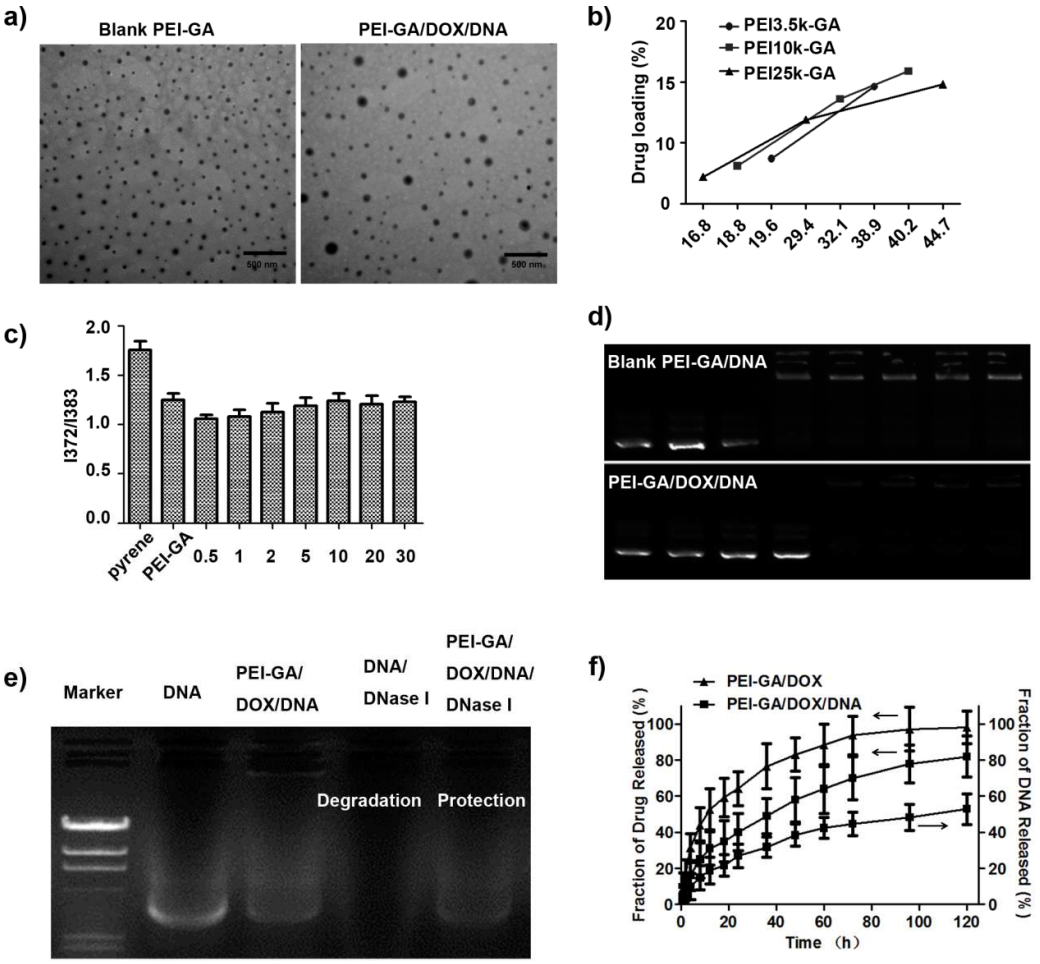

Figure. 2. The characterizations of the PEI-GA/DOX/DNA nanoparticles. (a) TEM image of blank and both DOX and shAkt1 loaded PEI-GA nanoparticles in saline solution (scale bar = 500 nm). (b) Drug loading of PEI-GA with different molecular weight of PEI and different graft ratio of GA. (c) Intensity ratios (I_{372}/I_{383}) of the emission spectra of pyrene, pyrene-loaded PEI-GA nanoparticles and pyrene-loaded PEI-GA/DNA complexes at the N/P ratios specified. (d) DNA binding ability of PEI-GA and DOX loaded PEI-GA nanoparticles (DNA, N/P ratios of 0.5, 1, 2, 5, 10, 20, and 30, respectively). (e) Protection study of DNA by agarose gel electrophoresis. (f) Release profile of PEI-GA/DOX and PEI-GA/DOX/shAkt1 in saline medium with 0.2 % Tween-80 at 37 ˚C (n=3).

One of the principal obstacles for impactful gene delivery is to prevent DNA from being degraded by enzymes *in vitro* and *in vivo*.[35, 36] An efficient delivery system

should be developed to avoid the degradation of DNA. The protection ability of PEI-GA/DOX/DNA (N/P ratio:10) against DNase I was evaluated by the retardation assay. As presented in Figure. 2e, naked DNA was totally degraded within 30 min incubation with DNase I, as evidenced by the disappearance of the bright band corresponding to free DNA. Whereas DNA in the complex was found to remain intact and the band was clear, which demonstrated that DOX loaded PEI-GA could protect DNA from degradation of DNase I effectively.

In vitro release of DOX and DNA from PEI-GA/DOX/DNA (N/P ratio:10) nanoparticles was shown in Figure. 2f. An obvious initial burst release of DNA is displayed in the first 12 h. It can be attributed to the release of some DNA bound weakly on the surface of the particles. In contrast, there is no initial burst release of DOX, suggesting that the chemical drug was well loaded in the cores of nanoparticls. . As indicated in Figure. 2f, PEI-GA/DOX nanoparticls demonstrated about 40% release of DOX over 8h, while PEI-GA/DOX released only 25 % at the same condition. The release of DOX from PEI-GA/DOX/DNA nanoparticles was relatively slower. This might be because of stronger hydrophobic interaction between GA with the DOX molecule or the electrostatic interaction of DNA and PEI to prevent the release of DOX when DNA is complexed with PEI-GA/DOX nanoparticles.

Cellular uptake and transfection studies. In order to achieve efficient transfection, it is integrant to develop a delivery system that will allow both chemical drug and gene across cell membrane.[7] Herein, we examined the effect of PEI-GA in mediating the uptake of DOX and DNA into HepG2 cells. As the intracellular fluorescence intensities varies directly as the internalized DOX, the cellular uptake of DOX was investigated using fluorescent inverted microscope. Clear red fluorescence of DOX was observed after 6 h transfection. PEI-GA/DOX/DNA group gave more detectable fluorescence in cells compared with the group treated with both PEI-GA/DOX/DNA complexes and GA or only DOX (Figure. 3a). As indicated in Figure. 3b, the value of the average fluorescence intensity of PEI-GA/DOX/DNA group detected by flow cytometer was remarkably greater than that of DOX and PEI-GA/DOX/DNA add GA groups, indicating that cellular uptake of

PEI-GA/DOX/DNA into HepG2 cells was highly influenced by GA moiety. Moreover, we performed the luciferase assay in line with the manufacturer's protocol to check transfection efficiency. The transfection efficiency was expressed in relative light units (RLU). As indicated in Figure. 3c, the transfection efficiency of luciferase of the PEI-GA/DOX /DNA complexes exhibited about five times as big as that of the PEI25k/DNA polyplexes. The results revealed that GA could functions effectively to mediated PEI-GA/DOX/DNA nanoparticles into cytoplasm, which might be due to the targeting ability of GA to liver tumor.[23-25, 29-31, 33] The high transfection efficiency of PEI-GA is fundamental for in vivo studies.

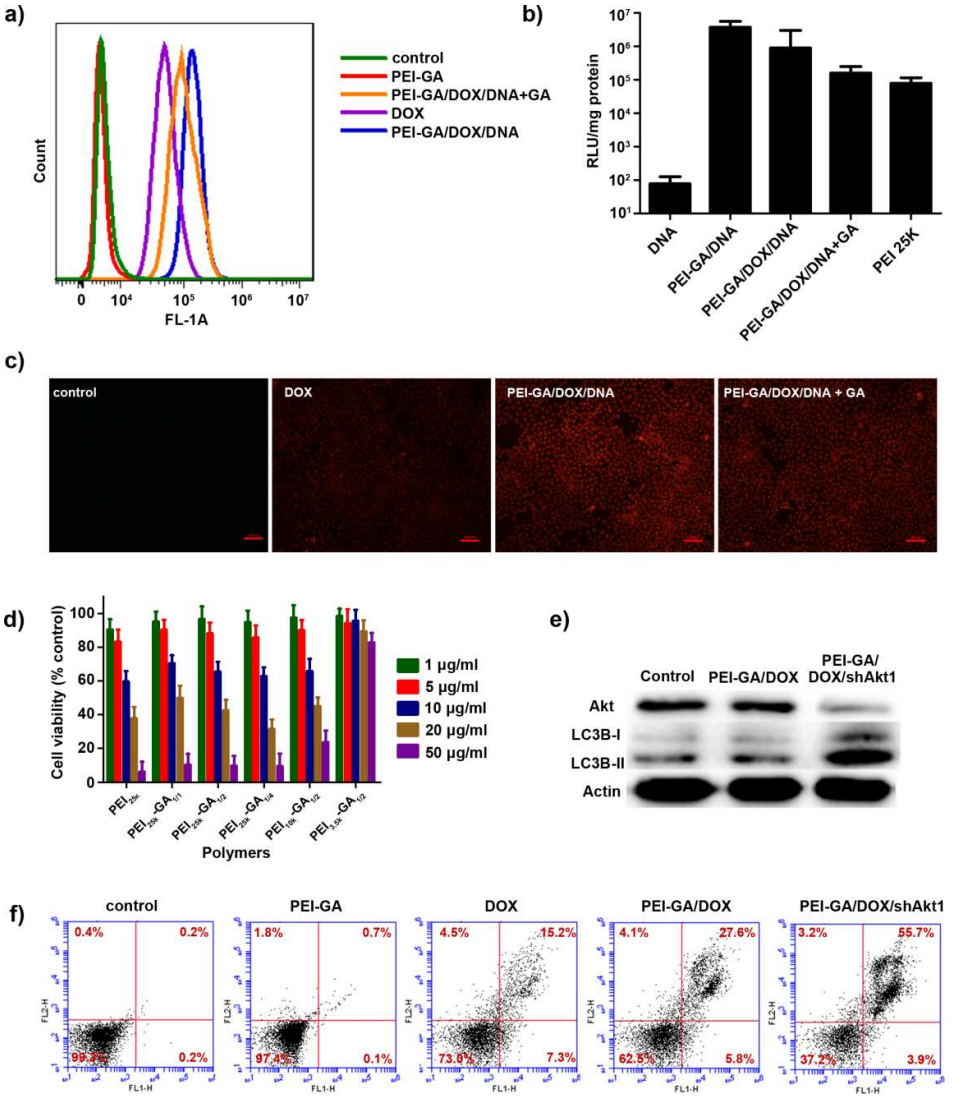

Figure. 3. (a) Flow cytometric analysis of fluorescence intensity of PEI-GA, DOX, PEI-GA/DOX/DNA+GA and PEI-GA/DOX/DNA nanoparticles treated cells. 10000

cells were counted and analyzed in each experiment. (b) Luciferase activity of DNA (pGL3-control), PEI25k, PEI-GA/DNA, PEI-GA/DOX/DNA and the combination of PEI-GA/DOX/DNA and GA. The experiments were confirmed three times. (c) Microscopic observations of DOX internalized in the HepG2 cells with treatment of DOX, PEI-GA/DOX/DNA+GA and PEI-GA/DOX/DNA (at a functional N/P ratio) following a 6 h period of incubation (scale bar = 100 μm). (d) In vitro cytotoxicities of PEI-GA with different molecular weight of PEI and graft ratio of GA at various concentrations at 24 h in the HepG2 cells. The experiments were confirmed three times. (e) Western blot analyses of Akt1, LC3B-I and LC3B-II proteins in HepG2 cells after incubation of PEI-GA/DOX and PEI-GA/DOX/shAkt1 formulations. (f) Apoptosis analysis of HepG2 cell line after treatment with PEI-GA, DOX, PEI-GA/DOX and PEI-GA/DOX/shAkt1, which was determined by Annexin V/propidium iodide staining.

In vitro cytotoxicity. Cytotoxicity is an important consideration for gene/drug carriers. Cytotoxicity of PEI-GA against HepG2 cells with different degrees of substitution and various concentrations was evaluated by MTS assay. As shown in Figure. 3d, PEI-GA conjugates showed higher biocompatibility with decreasing molecular weight of PEI and increasing degree of GA substitution. As $PEI_{3.5K}$-$GA_{1/2}$ was nontoxic even at 50 μg/mL during 24 h incubation time, so it may be a safe delivery carrier. This was probably attributed to its lower charge (19.9 mV) under physiological pH condition. The in vitro cytotoxicity of PEI3.5K-GA1/2 was determined in HepG2 cells using Light microscopic observation. The results indicated that the polymer displayed almost no cytotoxicity even at high concentrations (data not shown). The IC_{50} of free DOX, PEI-GA/DOX and PEI-GA/DOX/shAkt1 nanoparticles (N/P ratio:10) was estimated to be approximately 4.56, 2.07 and 0.99 μg/mL, respectively. The IC_{50} of PEI-GA/DOX/shAkt1 against HepG2 cells was 3.6-fold lower than that of free DOX. This enhanced inhibitory effect could be attributed to the combined therapy effect of DOX and shAkt1. For one thing, PEI-GA nanoparticles could deliver more amounts of DOX into HepG2 cells by comparison with free DOX solution. The phenomena were well matched with cellular uptake

study as shown in Figure. 3a and 3b. For another thing, there is a link between the activation of Akt kinase and human tumors,[37] and inhibition of the PI3-kinase-Akt signaling pathway by Akt1 shRNA might suppress the survival signal delivery that ultimately leads to the induction of apoptosis.[38] Therefore, it was reasonable to assume that PEI-GA/DOX/shAkt1 complexes could works as an efficient platform for cancer combination therapy.

Apoptosis and autophagy. After treatment in HepG2 cell line with PEI-GA/DOX/shAkt1 nanoparticles, cell growth slowed down, and furthermore the cells became more circular in shape and were progressively distorted. At 24 h after transfection with PEI-GA/DOX/shAkt1 nanoparticles, a marked decrease in the expression of the Akt1 protein was observed as shown in Figure. 3e. We also found that the expression of the protein of the cells treated with PEI-GA/DOX alone had almost no change compared with the control. Furthermore, it was amusing to observe that the transfection of PEI-GA/DOX/shAkt1 complexes up regulated the expression of autophagy-related LC3B-II protein. It was already reported that inhibition of Akt1 could induce autophagy[39] and autophagy constitutes an alternative pathway to cell death that is called type II cell death.[40] After treatment with PEI-GA/DOX/shAkt1 nanoparticles, the reduction of Akt1 protein level resulted in the up regulation of LC3B-II protein, which might significantly induce autophagy. High transfection of PEI-GA/DOX/shAkt1 nanoparticles in HepG2 cells (Figure. 3b) might be related with the low expression of Akt1 protein level (Figure. 3e). To further assess whether PEI-GA/DOX/shAkt1 complexes could efficiently induce apoptosis, results were observed using annexin V/PI double staining and the percentage of apoptosis was quantified. As indicated in Figure. 3f, when the HepG2 cell line was treated with DOX, PEI-GA/DOX, and PEI-GA/DOX/shAkt1, apoptosis was induced 15.2, 27.6 and 55.7 %, respectively, suggesting that apoptosis in HepG2 cells could be significantly enhanced by PEI-GA/DOX/shAkt1. In addition, apoptosis induction from PEI-GA was 0.7 %, similar to controls (0.2 %). This suggests that blank PEI-GA nanoparticles had no direct effect on apoptosis. The data achieved by apoptosis assay and cell growth inhibition experiment in the HepG2 cell line are in good accordance.

The apoptosis might be related with the induction of autophagy after the inhibition of the expression of Akt in the HepG2 cell line treated with PEI-GA/DOX/shAkt1 complexes.

Hemolysis test and systemic toxicity. The *in vivo* application of cationic polymers is often hindered by its nonspecific interactions with blood components. The compatibility of cationic vectors is a very important indicator for its introduction into the systemic circulation.[41] Figure. 4a displayed the effect of PEI-GA/DOX/DNA complexes on hemolytic activity at the functional N/P ratio. PEI_{25k}/DOX/DNA nanoparticles resulted in notable hemolysis, yet lower hemolysis was found in PEI-GA/DOX/DNA complex. Change in body weight and histological difference were investigated to evaluate systemic toxicity in mice. As indicated in Figure. 4b, the body weights of mice with PEI-GA nanoparticles treatment had no serious loss compared with saline treatment for a 2-week observation period, which suggested that no significant toxicity was induced by PEI-GA. There was also no obvious histological difference of major organs between the two groups (Figure. 4c). These findings suggested that PEI-GA is potential as an intravenous carrier for drug delivery.

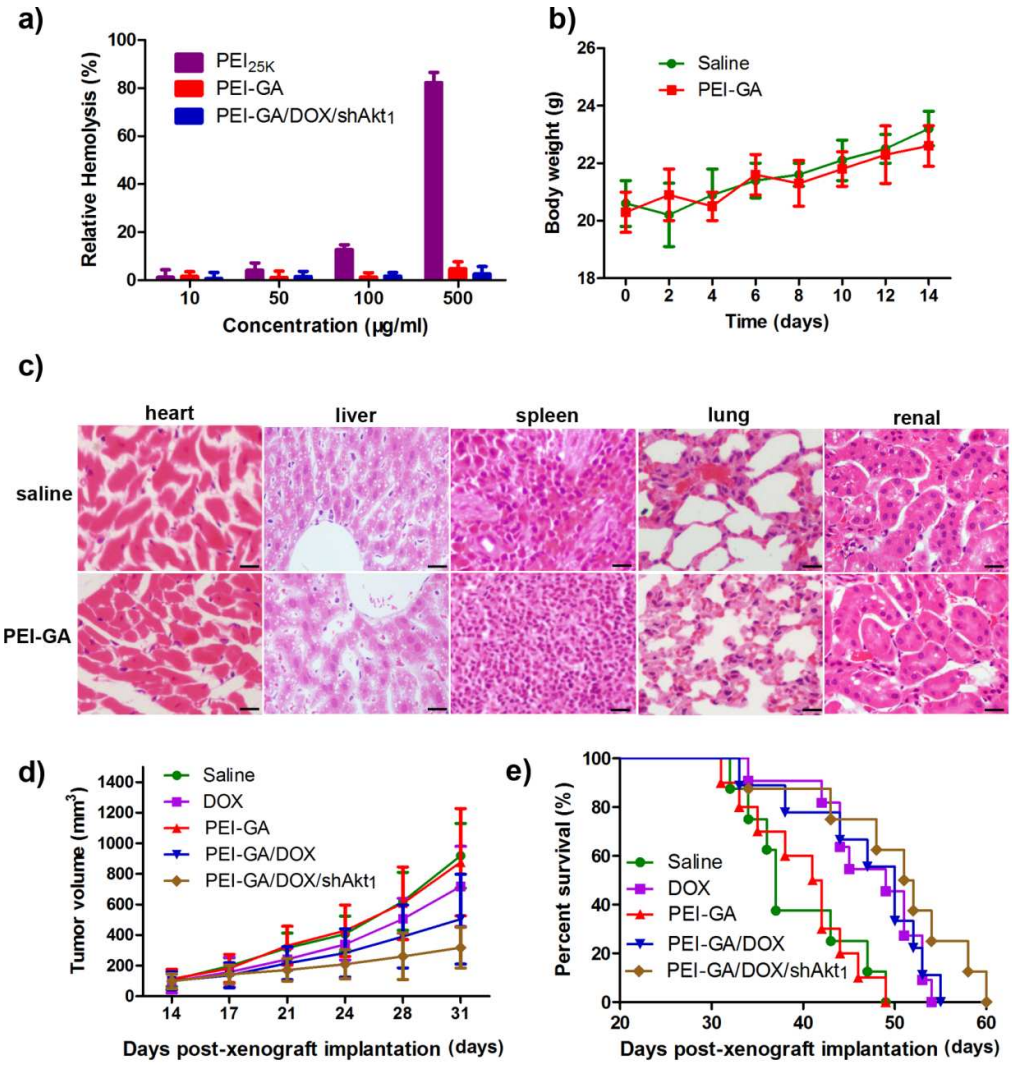

Figure. 4. (a) Hemolysis of PEI25k, PEI-GA and PEI-GA/DOX/shAkt1 at various concentrations. (b) Change in body weight. (c) Histological analysis for heart, liver, spleen, lung and kidney organs of mice at 16 days post intravenous injection of PEI-GA once a day (scale bar = 20 μm). (d) Tumor growth curves and (e) survival rates of saline, DOX, blank PEI-GA, PEI-GA/DOX and PEI-GA/DOX/shAkt1 formulations injected Hepa-1.6 tumor bearing mice.

In vivo antitumor assay in xenograft mice model. The effect of PEI-GA/DOX/shAkt1 complexes on tumor growth was investigated by in vivo tumor suppression experiment. Hepa-1.6 cells were inoculated subcutaneously in the C57BL-6J mice. As shown in Figure. 4d, we see no significant difference of tumor volume between the PEI-GA group and the control group. In contrast, the group

treated with PEI-GA/DOX/shAkt1 nanoparticles indicated outstanding growth inhibition of Hepa-1.6 cell grafted tumor-bearing C57BL-6J mice. Survival rate at the periods of time was indicated in Figure. 4e. Co-delivery of shAkt1 and DOX by PEI-GA was more powerful. According to reports, the efficacy of DOX in HCC is frequently not satisfactory, which may be associaited with the activation of Akt expression. RNA interference mediated by shRNA can specifically silence the targetd gene. In this case, combining DOX with shAkt could be a promising strategy for HCC therapy. To improve delivery to tumors, PEI-GA nanoparticls were developed and utilized. The application of PEI-GA/DOX/shAkt1 complexes has resulted in distinguished antitumor effect on the Hepa-1.6 tumor bearing mice. PEI-GA/DOX/shAkt1 complexes might provide a promising strategy for hepatic carcinoma therapy.

CONCLUSION

A low toxicity and high performance nanoparticle system was successfully constructed. PEI-GA with suitable graft ratio of GA can easily self-assemble into nano-aggregates based on the interaction of functional groups among GA. The graft of GA not only could markedly increase the transfection efficiency of PEI, but also could decrease the cytotoxicity of PEI. The formed nanoparticles showed suitable physicochemical properties to co-deliver gene/drug and effectively protected genes from degradation by enzyme. The IC_{50} of PEI-GA/DOX/shAkt1 against HepG2 cells was 3.6-fold lower than that of free DOX. In addition, better antitumor efficacy of PEI-GA/DOX/shAkt1 was observed on xenograft liver tumor. Therefore, PEI-GA/DOX/shAkt1 showed great potential in hepatic carcinoma therapy and the strategy of delivering chemotherapy drug and therapeutic genes using PEI-GA to simultaneously induce apoptosis and autophagy may represent a platform for future preclinical and clinical development.

AUTHOR INFORMATION

Corresponding Author

Professor Hu-Lin Jiang, E-mail: jianghulin3@163.com, Phone: +86-25-83271027, Fax: +86-25-83271027;

Professor Li Zong, E-mail: zong216@yahoo.com.cn, Phone: +86-25-83271317; Fax: +86-25-83271335.

Notes

The authors declare no competing financial interest.

Acknowledgements

This work was supported by the Funds for Creative Research Groups of China, National Natural Science Foundation of China (No. 81421005) and the Priority Academic Program Development of Jiangsu Higher Education Institutions (PAPD). Part of this work was supported by the Jiangsu Province Public Technology Service Center of Nanodrug Preparation and Evaluation. Part of this work was also supported by the National Natural Science Foundation of China (Grant No. 81573369 and 21301191), the Natural Science Foundation of Jiangsu Province (Grant No. BK20130661 and BK20140659). Part of this work was also supported by the Research Fund of the University of Macau (MYRG2015-00101-ICMS-QRCM). H.L. Jiang was supported by the Specially-Appointed Professors in Jiangsu Province Program.

References

1. Marquardt, J. U.; Thorgeirsson, S. S. SnapShot: Hepatocellular carcinoma. *Cancer Cell* **2014,** *25*, (4), e550.
2. Wang, L.; Lin, X.; Wang, J.; Hu, Z.; Ji, Y.; Hou, S.; Zhao, Y.; Wu, X.; Chen, C. Novel insights into combating cancer chemotherapy resistance using a plasmonic nanocarrier: enhancing drug sensitiveness and accumulation simultaneously with localized mild photothermal stimulus of femtosecond pulsed laser. *Adv Funct Mater* **2014,** *24*, (27), 4229-39.
3. Patil, Y. B.; Swaminathan, S. K.; Sadhukha, T.; Ma, L.; Panyam, J. The use of nanoparticle-mediated targeted gene silencing and drug delivery to overcome tumor drug resistance. *Biomaterials* **2010,** *31*, (2), 358-65.
4. Xu, Q.; Leong, J.; Chua, Q. Y.; Chi, Y. T.; Chow, P. K.-H.; Pack, D. W.; Wang, C.-H. Combined modality doxorubicin-based chemotherapy and chitosan-mediated p53 gene therapy using double-walled microspheres for treatment of human hepatocellular carcinoma. *Biomaterials* **2013,** *34*, (21), 5149-62.
5. Yang, Z.; Gao, D.; Cao, Z.; Zhang, C.; Cheng, D.; Liu, J.; Shuai, X. Drug and gene co-delivery systems for cancer treatment. *Biomater Sci* **2015,** *3*, (7), 1035-49.
6. Zhang, B. F.; Xing, L.; Cui, P. F.; Wang, F. Z.; Xie, R. L.; Zhang, J. L.; Zhang, M.; He, Y. J.; Lyu, J. Y.; Qiao, J. B.; Chen, B. A.; Jiang, H. L. Mitochondria apoptosis pathway synergistically activated by hierarchical targeted nanoparticles co-delivering siRNA and lonidamine. *Biomaterials* **2015,** *61*, 178-89.
7. Yin, T.; Wang, L.; Yin, L.; Zhou, J.; Huo, M. Co-delivery of hydrophobic paclitaxel and hydrophilic AURKA specific siRNA by redox-sensitive micelles for effective treatment of breast cancer. *Biomaterials* **2015,** *61*, 10-25.
8. Li, Y.; Xu, B.; Bai, T.; Liu, W. Co-delivery of doxorubicin and tumor-suppressing p53 gene using a POSS-based star-shaped polymer for cancer therapy. *Biomaterials* **2015,** *55*, 12-23.
9. Gandhi, N. S.; Tekade, R. K.; Chougule, M. B. Nanocarrier mediated delivery of siRNA/miRNA in combination with chemotherapeutic agents for cancer therapy:

current progress and advances. *J Controlled Release* **2014,** *194*, 238-56.

10. Jhaveri, A.; Deshpande, P.; Torchilin, V. Stimuli-sensitive nanopreparations for combination cancer therapy. *J Controlled Release* **2014,** *190*, 352-70.
11. Mao, Z.; Zhou, J.; Luan, J.; Sheng, W.; Shen, X.; Dong, X. Tamoxifen reduces P-gp-mediated multidrug resistance via inhibiting the PI3K/Akt signaling pathway in ER-negative human gastric cancer cells. *Biomed Pharmacother* **2014,** *68*, (2), 179-83.
12. Liu, Z.; Zhu, G.; Getzenberg, R. H.; Veltri, R. W. The Upregulation of PI3K/Akt and MAP Kinase Pathways is Associated with Resistance of Microtubule‐Targeting Drugs in Prostate Cancer. *J cell biochem* **2015,** *116*, (7), 1341-9.
13. Vivanco, I.; Sawyers, C. L. The phosphatidylinositol 3-Kinase AKT pathway in human cancer. *Nat Rev Cancer* **2002,** *2*, (7), 489-501.
14. Luo, J.; Manning, B. D.; Cantley, L. C. Targeting the PI3K-Akt pathway in human cancer: rationale and promise. *Cancer Cell* **2003,** *4*, (4), 257-62.
15. Jiang, H. L.; Xu, C. X.; Kim, Y. K.; Arote, R.; Jere, D.; Lim, H. T.; Cho, M. H.; Cho, C. S. The suppression of lung tumorigenesis by aerosol-delivered folate-chitosan-graft-polyethylenimine/Akt1 shRNA complexes through the Akt signaling pathway. *Biomaterials* **2009,** *30*, (29), 5844-52.
16. Jere, D.; Jiang, H. L.; Kim, Y. K.; Arote, R.; Choi, Y. J.; Yun, C. H.; Cho, M. H.; Cho, C. S. Chitosan-graft-polyethylenimine for Akt1 siRNA delivery to lung cancer cells. *Int J Pharm* **2009,** *378*, (1-2), 194-200.
17. Mao, Z.; Zhou, J.; Luan, J.; Sheng, W.; Shen, X.; Dong, X. Tamoxifen reduces P-gp-mediated multidrug resistance via inhibiting the PI3K/Akt signaling pathway in ER-negative human gastric cancer cells. *Biomed Pharmacother* **2014,** *68*, (2), 179-83.
18. Liu, Z.; Zhu, G.; Getzenberg, R. H.; Veltri, R. W. The Upregulation of PI3K/Akt and MAP Kinase Pathways is Associated with Resistance of Microtubule-Targeting Drugs in Prostate Cancer. *J Cell Biochem* **2015,** *116*, (7), 1341-9.

19. Fan, G.-C.; Zhou, X.; Wang, X.; Song, G.; Qian, J.; Nicolaou, P.; Chen, G.; Ren, X.; Kranias, E. G. Heat shock protein 20 interacting with phosphorylated Akt reduces doxorubicin-triggered oxidative stress and cardiotoxicity. *Circ Res* **2008,** *103*, (11), 1270-79.

20. Yin, H.; Kanasty, R. L.; Eltoukhy, A. A.; Vegas, A. J.; Dorkin, J. R.; Anderson, D. G. Non-viral vectors for gene-based therapy. *Nat Rev Genet* **2014,** *15*, (8), 541-55.

21. Chen, Y.; Gao, D. Y.; Huang, L. In vivo delivery of miRNAs for cancer therapy: challenges and strategies. *Adv Drug Deliv Rev* **2015,** *81*, 128-41.

22. Kurisawa, M.; Yokoyama, M.; Okano, T. Gene expression control by temperature with thermo-responsive polymeric gene carriers. *J Controlled Release* **2000,** *69*, (1), 127-37.

23. Tian, Q.; Zhang, C. N.; Wang, X. H.; Wang, W.; Huang, W.; Cha, R. T.; Wang, C. H.; Yuan, Z.; Liu, M.; Wan, H. Y.; Tang, H. Glycyrrhetinic acid-modified chitosan/poly(ethylene glycol) nanoparticles for liver-targeted delivery. *Biomaterials* **2010,** *31*, (17), 4748-56.

24. Zhang, C.; Wang, W.; Liu, T.; Wu, Y.; Guo, H.; Wang, P.; Tian, Q.; Wang, Y.; Yuan, Z. Doxorubicin-loaded glycyrrhetinic acid-modified alginate nanoparticles for liver tumor chemotherapy. *Biomaterials* **2012,** *33*, (7), 2187-96.

25. Cheng, M.; Xu, H.; Wang, Y.; Chen, H.; He, B.; Gao, X.; Li, Y.; Han, J.; Zhang, Z. Glycyrrhetinic acid-modified chitosan nanoparticles enhanced the effect of 5-fluorouracil in murine liver cancer model via regulatory T-cells. *Drug Des Devel Ther* **2013,** *7*, 1287-99.

26. Bajaj, A.; Kondaiah, P.; Bhattacharya, S. Synthesis and gene transfection efficacies of PEI-cholesterol-based lipopolymers. *Bioconjug Chem* **2008,** *19*, (8), 1640-51.

27. Liu, Z.; Zhang, Z.; Zhou, C.; Jiao, Y. Hydrophobic modifications of cationic polymers for gene delivery. *Prog Polym Sci* **2010,** *35*, (9), 1144-62.

28. Park, K. M.; Kang, H. C.; Cho, J. K.; Chung, I.-J.; Cho, S.-H.; Bae, Y. H.; Na, K. All-trans-retinoic acid (ATRA)-grafted polymeric gene carriers for nuclear translocation and cell growth control. *Biomaterials* **2009,** *30*, (13), 2642-52.

29. Li, J.-y.; Cao, H.-y.; Liu, P.; Cheng, G.-h.; Sun, M.-y. Glycyrrhizic acid in the treatment of liver diseases: literature review. *Biomed Res Int* **2014,** *2014*.

30. Zhang, L.; Yao, J.; Zhou, J.; Wang, T.; Zhang, Q. Glycyrrhetinic acid-graft-hyaluronic acid conjugate as a carrier for synergistic targeted delivery of antitumor drugs. *Int J Pharm* **2013,** *441*, (1), 654-64.

31. Huang, W.; Wang, W.; Wang, P.; Tian, Q.; Zhang, C.; Wang, C.; Yuan, Z.; Liu, M.; Wan, H.; Tang, H. Glycyrrhetinic acid-modified poly (ethylene glycol)–b-poly (γ-benzyl l-glutamate) micelles for liver targeting therapy. *Acta biomater* **2010,** *6*, (10), 3927-35.

32. Jiang, H. L.; Kwon, J. T.; Kim, E. M.; Kim, Y. K.; Arote, R.; Jere, D.; Jeong, H. J.; Jang, M. K.; Nah, J. W.; Xu, C. X.; Park, I. K.; Cho, M. H.; Cho, C. S. Galactosylated poly(ethylene glycol)-chitosan-graft-polyethylenimine as a gene carrier for hepatocyte-targeting. *J Control Release* **2008,** *131*, (2), 150-7.

33. Tian, Q.; Wang, X. H.; Wang, W.; Zhang, C. N.; Wang, P.; Yuan, Z. Self-assembly and liver targeting of sulfated chitosan nanoparticles functionalized with glycyrrhetinic acid. *Nanomedicine* **2012,** *8*, (6), 870-9.

34. Park, H. J.; Yang, F.; Cho, S. W. Nonviral delivery of genetic medicine for therapeutic angiogenesis. *Adv Drug Deliv Rev* **2012,** *64*, (1), 40-52.

35. Jiang, H. L.; Xu, C. X.; Kim, Y. K.; Arote, R.; Jere, D.; Lim, H. T.; Cho, M. H.; Cho, C. S. The suppression of lung tumorigenesis by aerosol-delivered folate-chitosan-graft-polyethylenimine/Akt1 shRNA complexes through the Akt signaling pathway. *Biomaterials* **2009,** *30*, (29), 5844-52.

36. Wang, F. Z.; Xie, Z. S.; Xing, L.; Zhang, B. F.; Zhang, J. L.; Cui, P. F.; Qiao, J. B.; Shi, K.; Cho, C. S.; Cho, M. H.; Xu, X.; Li, P.; Jiang, H. L. Biocompatible polymeric nanocomplexes as an intracellular stimuli-sensitive prodrug for type-2 diabetes combination therapy. *Biomaterials* **2015,** *73*, 149-59.

37. Xiang, T.; Jia, Y.; Sherris, D.; Li, S.; Wang, H.; Lu, D.; Yang, Q. Targeting the Akt/mTOR pathway in Brca1-deficient cancers. *Oncogene* **2011,** *30*, (21), 2443-50.

38. Dienstmann, R.; Rodon, J.; Serra, V.; Tabernero, J. Picking the point of

inhibition: a comparative review of PI3K/AKT/mTOR pathway inhibitors. *Mol Cancer Ther* **2014,** *13*, (5), 1021-31.

39. Lee, C. H.; Lin, S. T.; Liu, J. J.; Chang, W. W.; Hsieh, J. L.; Wang, W.-K. Salmonella induce autophagy in melanoma by the downregulation of AKT/mTOR pathway. *Gene ther* **2014,** *21*, (3), 309-16.
40. Gozuacik, D.; Kimchi, A. Autophagy as a cell death and tumor suppressor mechanism. *Oncogene* **2004,** *23*, (16), 2891-906.
41. Rekha, M.; Sharma, C. P. Blood compatibility and in vitro transfection studies on cationically modified pullulan for liver cell targeted gene delivery. *Biomaterials* **2009,** *30*, (34), 6655-64.

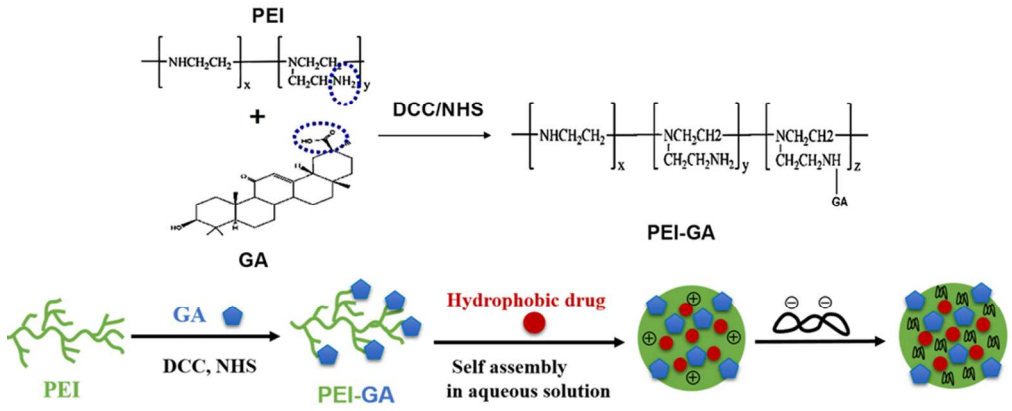

Poly(ethylenimine)-glycyrrhetinic acid nanoparticles loaded with doxorubicin and shAkt1
88x35mm (300 x 300 DPI)